



## Improving Thermo-hydraulic Performance of Parallel-plate Flow with a Particular Counter-current Flow Division

M. Goodarzi\*, N. Eshghabadi, R. Sadeghi

Faculty of Engineering, Bu-Ali Sina University, Hamedan, Iran

**ABSTRACT:** A particular counter-current flow division has been introduced to improve the thermal and hydraulic performances of flow through two isotherm parallel plates. It has been constructed by inserting two zero thickness and impermeable flat plates within the parallel-plate channel to establish a central and two external sub-channels. The total flow rate has been subdivided into two streams for supplying into the central and two external sub-channels in counter-current directions. The effect of the cross-section ratio on the thermal and hydraulic performances has been investigated for two flow division regimes. The obtained results showed that better thermal performance could be enhanced when the cross-section of the central sub-channel was greater than the external ones. Regarding the overall performance, it has been concluded that the best performance could be enhanced when the flow and cross-section were equally subdivided. In this particular case, the percent of the heat transfer enhancement compared to the single-pass channel was 50%. Meanwhile, the power consumption increment of the proposed flow arrangement significantly decreased compared to the two previously proposed double-pass arrangements. It seems that the proposed flow arrangement is a better alternative for double-pass arrangement.

### Review History:

Received: Dec. 24, 2018  
Revised: Apr. 25, 2019  
Accepted: May, 05, 2019  
Available Online: May, 07, 2019

### Keywords:

Parallel-plate flow  
Heat transfer  
Uniform wall temperature  
Counter-current  
Cross-section ratio

## 1- INTRODUCTION

Heat transfer between the fluid flow and two parallel plates is a benchmark problem, which has been frequently investigated [1]. Many compact heat exchangers contain numerous flow structures within the parallel plates. Therefore, despite the simplicity of the flow structure within the parallel-plate channel, it remains an important heat transfer problem from the practical viewpoint.

The simplified model for this particular heat transfer problem is known as the classic Graetz problem [2,3] in which the axial conduction is negligible and the flow regime is laminar. But the axial conduction significantly affects the temperature distribution when the Prandtl number of the fluid flow is low. When considering the axial conduction within the parallel-plate flow, it is known as the extended Graetz problem [4-7].

The rate of the heat transfer depends on the temperature difference between the fluid flow and channel walls, the surface of the heat transfer, and also the convective heat transfer coefficient [1]. The convective heat transfer coefficient depends on the flow pattern through the parallel-plate channel. This coefficient has been frequently measured in research studies for different flow patterns [8-10].

In practice, there are some occupation restrictions for installing the parallel-plate channels. In this case, the external surface of the parallel-plate channel is fixed and the only

solution for increasing the surface of heat transfer is to use the internally finned type channels [11,12]. The main deficiency of the internally finned wall for the parallel-plate channel is the deposition of the suspended particles on the fins, which gradually increases the blockage against the flow and thermal resistance. A wavy channel wall is another solution with a less unfavorable deposition effect [13-15].

An alternative proposal for improving the thermal performance of a parallel-plate flow with a restriction on the occupation space is to change the flow passage. Ho et al. [16-19] inserted a flat plate with a negligible thickness between the two main walls of the parallel-plate channel to provide two sub-channels. The flow enters the incoming sub-channel and then returns to the outgoing sub-channel. Both incoming and outgoing flows exchange the heat with each other as well as do with the channel walls. Ho et al. [16-19] showed that doubling the flow passage within the parallel-plate channel increased the thermal performance. Goodarzi and Mazharmanesh [20] used a sinusoidal separating plate within the double-pass parallel-plate channel to improve the thermal performance of the channel a little. Ho et al. [21,22] also studied the multi-pass flow arrangement within the parallel-plate channel. They reported slightly more heat transfer enhancement compared to the double-pass arrangement, but with significantly greater power consumption for pumping the flow through the sub-channels.

Goodarzi and Nouri [23] proposed a new flow passage

\*Corresponding author's email: m.goodarzi@basu.ac.ir



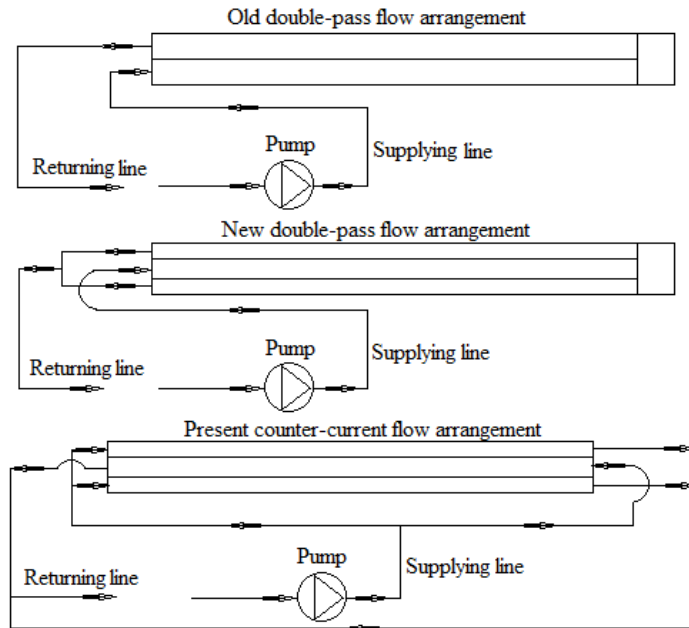


Fig. 1. Schematics of the present counter-current and two double-pass flow arrangements

within the parallel-plate channel. It is schematically shown in Fig. 1 in comparison to the old double-pass channel flow. The total mass-flow rate entered to the central sub-channel and then equally divided to the two streams returning to the two external sub-channels. They showed that this particular flow arrangement provided better wall temperature uniformity. There are other recently published articles investigating the thermal performance of the old double-pass channel flow (see Fig.1) under different thermal boundary conditions. But, the authors decided to address the main and original relevant references in the present article.

The total flow rate passes through each sub-channel of the previously proposed double-pass flow arrangements [16-23]. Therefore, the power consumption for supplying the flow rate increases rapidly compared to the single-pass arrangement and It is not favorable from the cost and energy viewpoints. A particular flow division is proposed in the present study to decrease power consumption. This particular flow arrangement is shown in Fig.1 in comparison to the two mentioned double-pass arrangements. The present proposed flow arrangement has never been introduced, studied, and investigated before. Therefore, the main objective of the present study is to introduce a new flow arrangement within the parallel-plate channel for decreasing the power consumption compared to the previous double-pass arrangements. The thermal performance of the proposed flow arrangement should be analyzed by measuring the heat transfer enhancement compared to the single-pass flow arrangement. The results of the present study may encourage the engineers for using the proposed counter-current flow division within the compact flat plate heat exchangers.

## 2- PROBLEM DEFINITION

The benchmark problem is a laminar flow between two

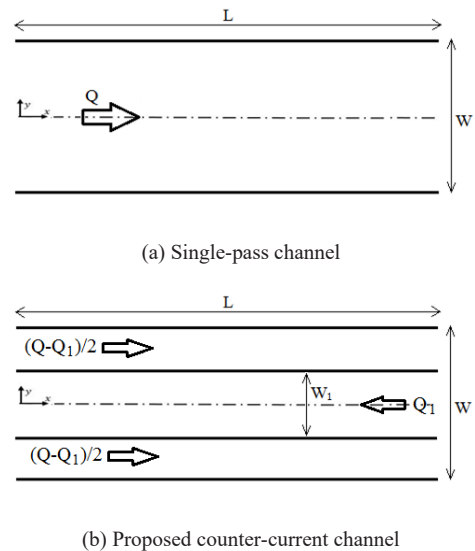


Fig. 2. Schematics of the single-pass and the proposed counter-current channels

parallel plates, which is referred to as a single-pass channel. The temperatures of the two parallel plates are the same and uniform. Fig. 2(a) shows the geometrical dimensions of the single-pass channel. The ratio of the length to the width of the channel is 120. By symmetrically inserting two zero thickness plates between the main parallel plates, a new counter-current flow arrangement is constructed without changing the external dimensions. The total flow rate is subdivided into two streams one of them is supplied to the central sub-channel, while the remaining one is equally supplied to the two external sub-channels in the counter-current directions. Fig. 2(b) schematically shows the new counter-current flow arrangement.

The thermo-flow regime within the channel is usually characterized by Graetz number, which is described as

$$Gz = RePr \frac{W}{L} \tag{1}$$

where, Re and Pr are Reynolds number and Prandtl number, respectively. Reynolds number is defined as

$$Re = \frac{\rho UW}{\mu} \tag{2}$$

where U is the averaged velocity of the flow rate within the single-pass arrangement, and  $\rho$  and  $\mu$  are density and dynamic viscosity of the fluid, respectively. The flow regime within the sub-channels of the new counter-current channel and also single-pass one is laminar, when Prandtl number is in order of 1 and Graetz number is less than 1000.

For generalizing the results, the dependent and independent variables are reported in dimensionless forms. Dimensionless length and temperature are defined as

$$\xi = \frac{x}{L} \tag{3}$$

$$\theta = \frac{T - T_i}{T_w - T_i} \tag{4}$$

where, T,  $T_w$ , and  $T_i$  denote the temperatures of the fluid flow, walls, and inlet flow, respectively. The cross-section ratio is also defined as

$$K = \frac{W_1}{W} \tag{5}$$

The total flow rate is subdivided to the two ones. Two flow division regimes are used. In the flow division regime 1, the total flow rate is equally subdivided into two streams: one of them is supplied to the internal sub-channel and the other one is equally supplied to the external sub-channels ( $Q_1=Q/2$ ). In the flow division regime 2, each subdivided flow rate is proportional to the cross-section area of the corresponding sub-channel ( $Q_1=KQ$ ). Therefore, the flow division regimes 1 and 2 are the same for cross-section ratio of  $K=0.5$ .

### 3- GOVERNING EQUATION AND BOUNDARY CONDITIONS

The width between the two parallel plates is small compared to the plate length; therefore, the flow regime within the parallel-plate channel is assumed to be laminar and incompressible. The process of the heat transfer from the walls to the fluid flow is steady-state. All flows within the sub-channels are hydraulically fully-developed. Hence, the energy equation governs the problem completely. The energy equation can be presented in the vector form as

$$\rho c_p (\vec{V} \cdot \vec{\nabla}) T = k \nabla^2 T \tag{6}$$

where,  $\vec{V}$ , k, and  $c_p$  are velocity vector, thermal

conductivity, and thermal capacity of the fluid, respectively.

The flows enter the sub-channels with the uniform temperature, i.e.  $T_i$ . Two main parallel plates have the same uniform temperature, i.e.  $T_w$ . There is no need for applying a particular thermal boundary condition on the impermeable separating plate because it is a zero thickness plate. It means the temperature and its gradient are continues across the separating plate. Since the flow field and all hydraulic and thermal boundary conditions are symmetric with respect to the centerline, it is better to simulate one-half of the flow field; therefore, all gradients of the dependent variables normal to the symmetry plane are set to zero.

### 4- Details of the numerical method

There is a complicated analytical solution for this particular heat transfer problem. But, for avoiding the analytical singularities at the edge points [24], a simplified numerical procedure based on the finite volume method was used to compute the temperature distribution within the flow field [25]. A structured grid system was used to discretize the flow field. A second-order upwind scheme was used to discretize the convective term, while a central scheme was used to discretize the conductive terms [25]. The resulted system of the algebraic equations was implicitly solved using an iterative procedure until the temperature distribution reached its numerically invariant level over the grid system. A FORTRAN program was developed for this purpose.

### 5- Grid independency test

To be sure the computed results are independent of the grid system, several grid systems were used for each case study. The finalized grid system was selected when a distributed parameter such as local temperature profile was not dependent on the grid system. For example, Fig.3 shows

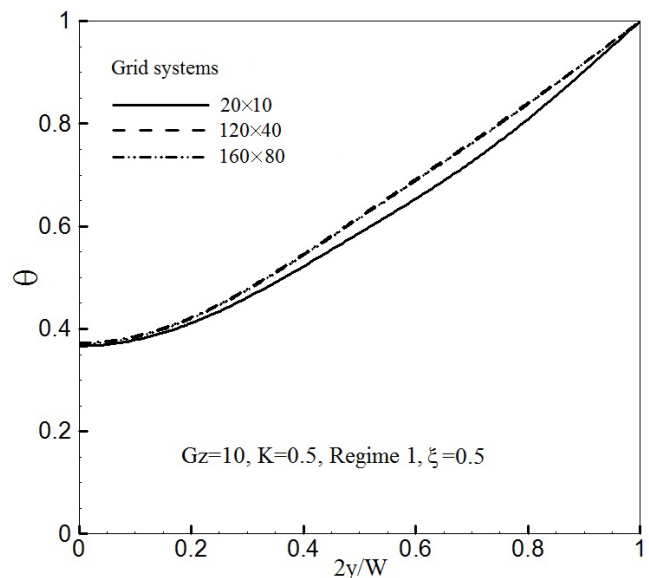


Fig. 3. Dimensionless temperature profiles at the middle section of the counter-current channel corresponding to the three different grid systems

the three computed temperature profiles at the middle section of the counter-current channel with  $K=0.5$  corresponding to the three different grid systems when  $Gz=10$ . It illustrates that the computed temperature profiles for this particular case study are the same for two grid systems with  $120 \times 40$  and  $160 \times 80$  grid numbers.

**6- Validation**

The local Nusselt number is defined as

$$Nu = \frac{hW}{k} = \frac{Wq_w^*}{k(T_w - T_m)} \tag{7}$$

where,  $q_w^*$  and  $T_m$  are the local heat flux and average temperature of the flow, respectively. The local heat flux is computed as

$$q_w^* = k \frac{\partial T}{\partial y} \tag{8}$$

A flow field with a low Graetz number provides the thermally fully developed condition at the downstream. To validate the applied numerical method, the local Nusselt number has been computed at the far downstream of the single-pass channel for two different thermal boundary conditions of uniform wall temperature and uniform heat flux. The computed values for these well-known thermal boundary conditions are compared with the analytical results [26] in Table 1. There are very good agreements between the numerical and analytical results. For each thermal boundary condition, the difference between the numerical and analytical results is less than 1%.

**7- Results and discussions**

**7-1- Heat transfer and temperature distribution**

The best parameter for measuring the heat transfer enhancement is the local Nusselt number. The entrance of the single-pass channel is allocated at  $x=0$  so is the entrance of the sub-channel of the counter-current channel. Fig 4 shows the variations of the local Nusselt numbers of the single-pass and three typical proposed counter-current channels for two mentioned flow division regimes and different flow rates, i.e. different Graetz numbers. An overall inspection illustrates that the local Nusselt number of the counter-current channel varies as the single-pass channel does. It is, the local Nusselt number rapidly decreases at the channel entrance and then asymptotically decreases to some invariant value. The local Nusselt number of the counter-current channel at the entrance of the external sub-channel is always greater than the single-pass one. Fig.4 shows that the local Nusselt number of the counter-current channel usually remains greater than

the single-pass channel at the downstream, except for the low flow rate ( $Gz=10$ ).

From a geometrical viewpoint, Fig. 4 illustrates that at a high flow rate, the local Nusselt number of the counter-current channel with a greater cross-section ratio is higher than the other ones regardless of the flow division regime. This conclusion deteriorates at the downstream of the external sub-channel for low flow rate. At high flow rates, i.e.  $Gz > 100$ , the local Nusselt number of the counter-current channel with  $K=0.7$  and regime 1 is greater than the other ones throughout the flow passage, while that with  $K=0.3$  and regime 2 possesses the least local Nusselt number among the other ones. The differences among the values of the local Nusselt numbers corresponding to the three cross-section ratios with regime 2 are less than those in regime 1.

The local Nusselt number is inversely proportional to the local thickness of the thermal boundary layer. Note that when inserting a plate within the single-pass channel while the average velocity is the same as that within the single-pass channel (flow division regime 1) or greater (flow division regime 2), maximum of the velocity profile within the external sub-channel increases. It consequently increases the local Reynolds number near the channel wall and decreases the rate of the growth of the thermal boundary layer. Therefore, the following discussions are devoted to investigating the thermal boundary layer by considering the temperature distribution within the flow field.

Fig.5 shows the contours of the dimensionless temperature throughout the single-pass channel and also two typical counter-current channels with two particular flow division regimes and  $Gz=10$ . Looking at the entrances of the channels, it is obvious that the thickness of the thermal boundary layer becomes thinner when using the proposed counter-current channel compared to the single-pass flow arrangement. The thinnest thermal boundary layer at the entrance region is corresponding to the cross-section ratio of  $K=0.7$  and flow division regime 1, which leads to the highest local Nusselt number as was mentioned in Fig. 4. But, the thermal boundary layer thickness of the counter-current channel is slightly greater than the single-pass channel at the downstream, except for the exit plane corresponding to the entrance of the internal sub-channel. The low-temperature flow enters the internal sub-channel and re-thins the thermal boundary layer. It slightly increases the local Nusselt number. Note that the re-thinning of the thermal boundary layer is more sensible for cross-section ratio of  $K=0.7$ , because of entering the more cooling flow rate to the internal sub-channel.

Fig. 6 shows the temperature distribution within the channels at the flow rate corresponding to  $Gz=100$ .

**Table 1. Comparison between the numerical and analytical values of the thermally fully developed Nusselt number for two different thermal boundary conditions**

Thermal boundary condition	Analytical results [26]	Present study
Uniform heat flux	4.12	4.10
Uniform wall temperature	3.72	3.68

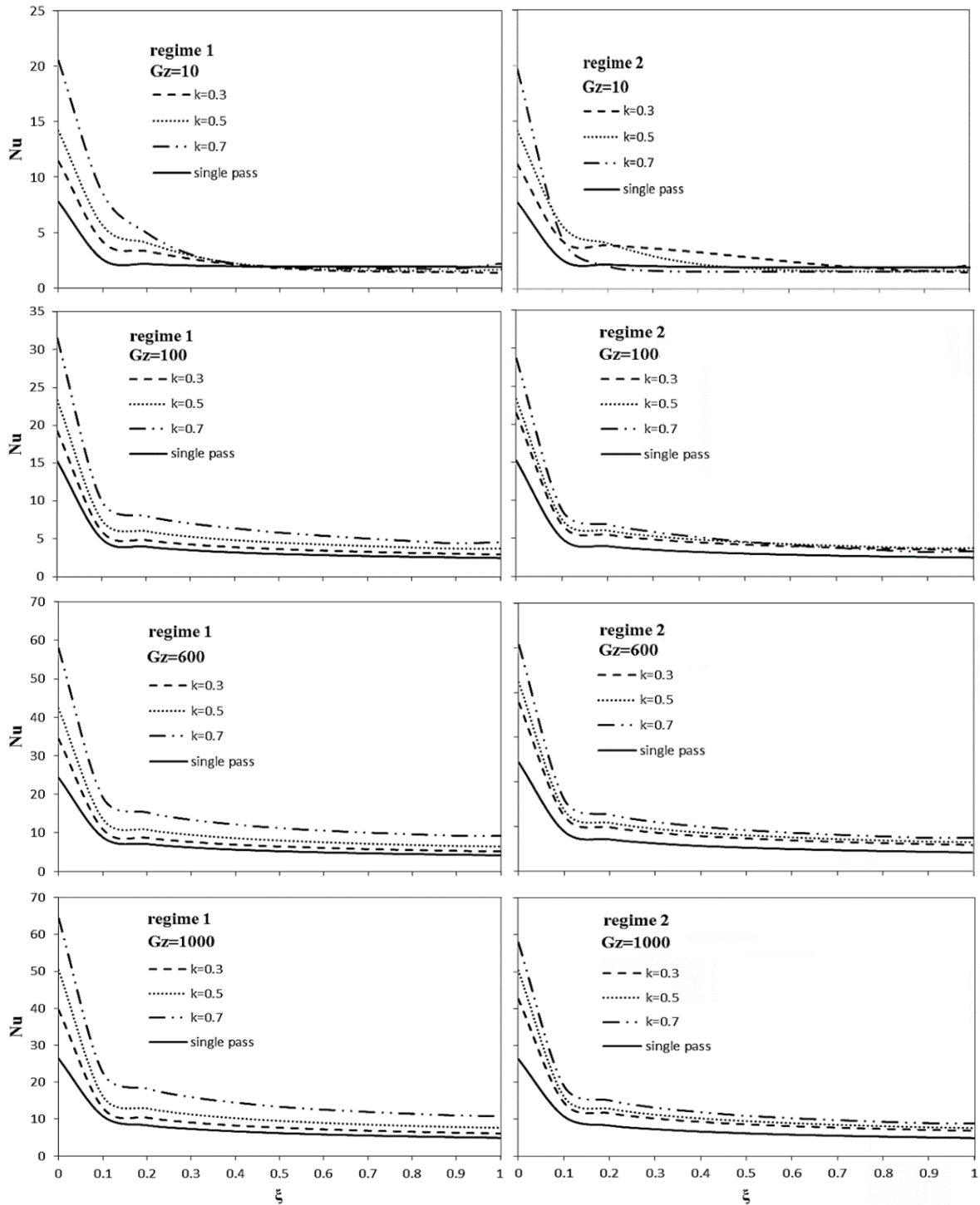


Fig. 4. Local Nusselt number along the different channels with various flow rates

Comparison between Figs. 5 and 6 demonstrates that the thermal boundary layer slightly diffuses to the central core both in the single-pass and counter-current channels. Note that in the counter-current channel with cross-section ratio of  $K=0.3$ , the thermal boundary layer does not diffuse to the flow within the internal sub-channel. Therefore, like the single-pass channel, the thermal boundary layer thickness in this particular cross-section ratio increases monotonically

to the downstream. In fact, the counter-current flow within the internal sub-channel just decreases the growing rate of the thermal boundary layer compared to the single-pass flow arrangement. But, for the cross-section ratio of  $K=0.7$ , the thermal boundary layer diffuses to the flow within the internal sub-channel. Therefore, the flow within the internal sub-channel can re-thin the thermal boundary layer at the exit plane and increases the local Nusselt number.

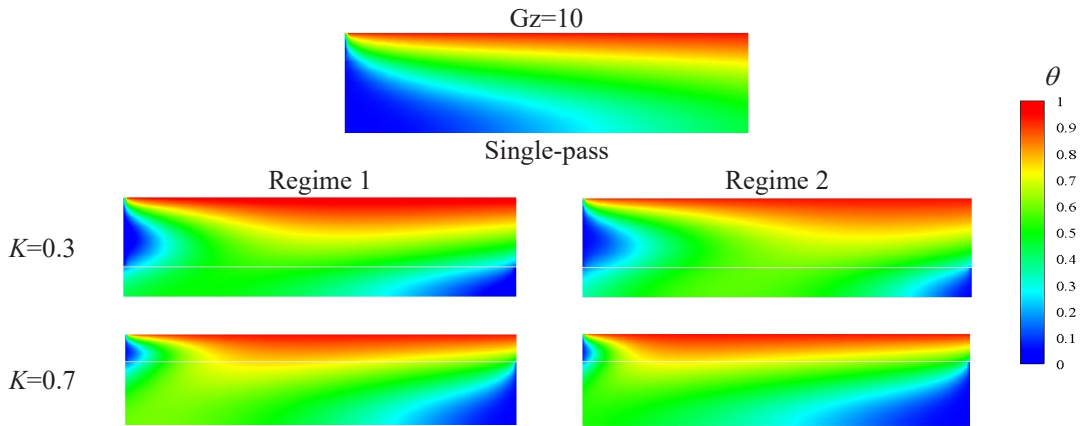


Fig. 5. Temperature distributions within the single-pass and two different counter-current channels for a flow rate corresponding to  $Gz=10$

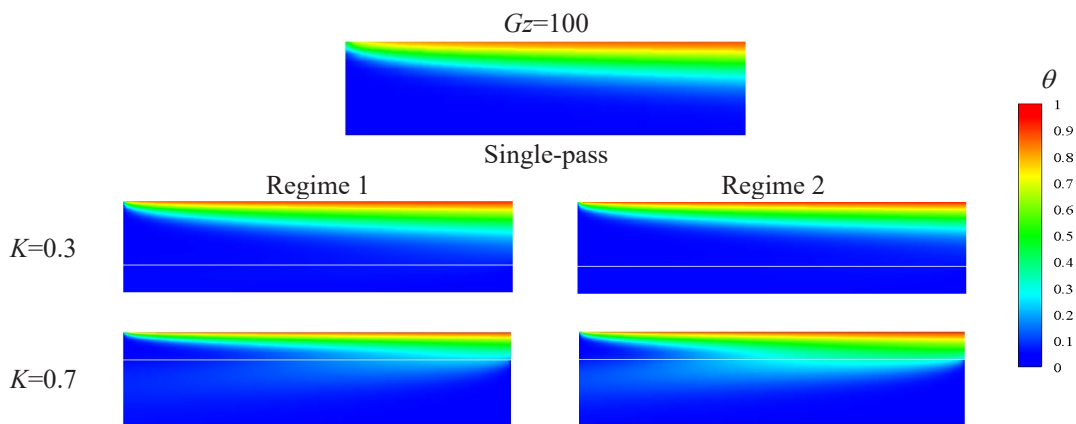


Fig. 6. Temperature distributions within the single-pass and two different counter-current channels for a flow rate corresponding to  $Gz=100$

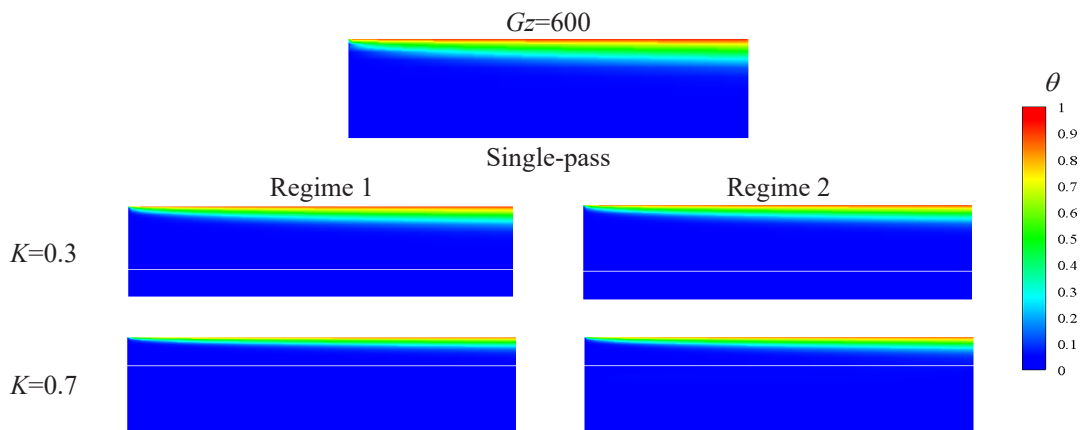


Fig. 7. Temperature distributions within the single-pass and two different counter-current channels for a flow rate corresponding to  $Gz=600$

Referring to Fig.6, it is clear that the thermal boundary layer thicknesses in all counter-current arrangements are smaller than that in the single-pass channel. Besides, the thermal boundary layer thickness of the counter-current channel

with cross-section ratio of  $K=0.7$  and flow division regime 1 is thoroughly smaller than the other counter-current flow arrangements.

Figs. 7 and 8 show the temperature distributions within

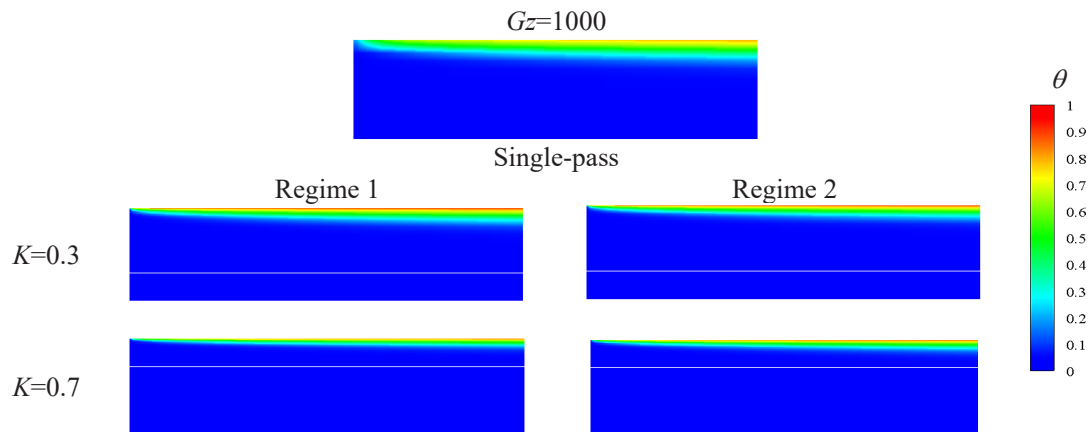


Fig. 8. Temperature distributions within the single-pass and two different counter-current channels for a flow rate corresponding to  $Gz=1000$

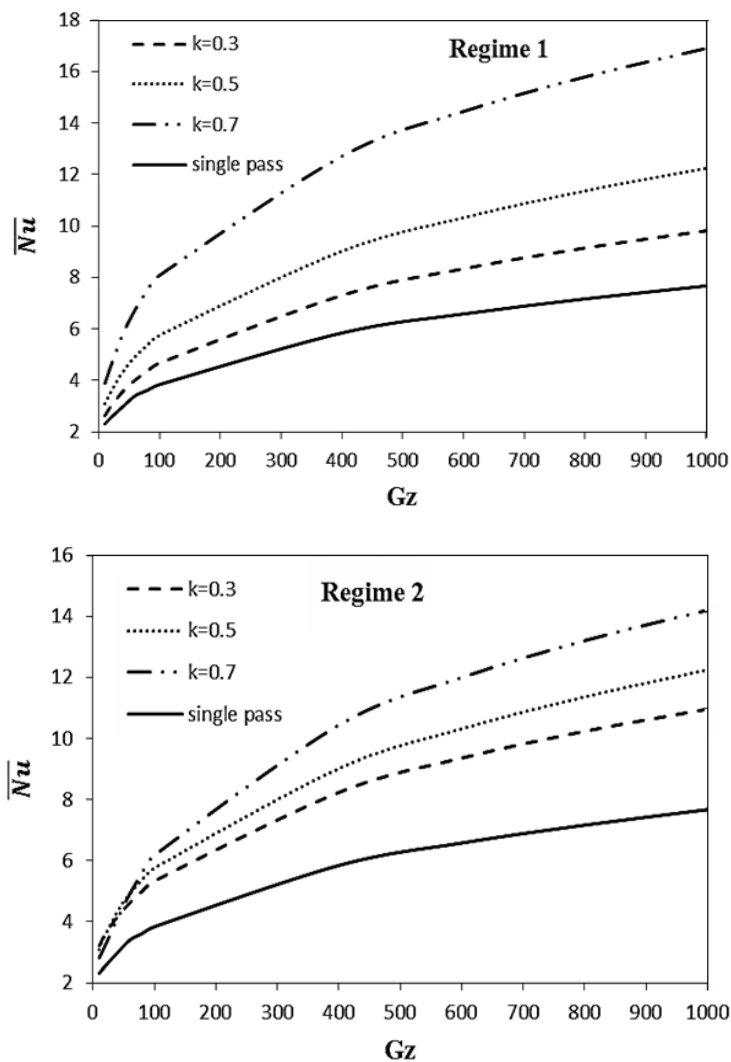


Fig. 9. Average Nusselt number versus the Graetz number for different channels

the channels at two higher flow rates, i.e.  $Gz=600$  and  $1000$ , respectively. These Figures show that the thermal boundary layer does not diffuse to the flow within the internal sub-channel for all cross-section ratios and flow division regimes. Therefore, there is no effect of re-thinning the thermal

boundary layer in these particular flow rates. The only effect of the counter-current flow within the internal sub-channel is to decrease the growing rate of the thermal boundary layer compared to the single-pass channel. Of course, this effect is more significant for the cross-section ratio of  $K=0.7$  when

using the flow division regime 1.

**7-2- Heat transfer enhancement**

The above-mentioned discussions on the temperature distributions within the channels declare that the proposed counter-current flow arrangement could decrease the growing rate of the thermal boundary layer regardless of the cross-section ratio, the flow division regime, and the flow rate. But, at a low flow rate, when the thermal boundary layer can diffuse to the flow within the internal sub-channel, the counter-current flow within the internal sub-channel can re-thin the thermal boundary layer at the end of the external sub-channel.

Now, some integrated parameters can be calculated for quantitative comparisons. The average Nusselt number is computed as

$$\bar{Nu} = \frac{1}{L} \int_0^L Nu dx \tag{9}$$

Then, the enhanced heat transfer using the proposed counter-current flow arrangement is introduced as

$$E_Q = \frac{\bar{Nu}_{cc} - \bar{Nu}_s}{\bar{Nu}_s} \tag{10}$$

where, indices  $_{cc}$  and  $_s$  refer to counter-current and single-pass flow arrangements, respectively.

Fig. 9 shows the average Nusselt numbers of all flow arrangements based on the Graetz number. This Figure shows that the average Nusselt number increases as the Graetz Number increases for all cross-section ratios and two flow division regimes. Note that as was already mentioned, the two flow division regimes are the same when the cross-section ratio is  $K=0.5$ . It helps us compare the thermal performances of the other flow regimes and cross-section ratios with this particular case and also single-pass arrangement. Considering Fig. 9, it is clear that the average Nusselt number of the counter-current channel with cross-section ratio of  $K=0.7$  and flow division regime 1 is always the best case among the other

channels.

Fig. 10 shows the enhanced heat transfer when using the proposed counter-current flow arrangement. This Figure illustrates that the heat transfer enhancement of the counter-current flow arrangement increases rapidly by increasing the Graetz number in the range of the low flow rates and then asymptotically increases to some invariant values depending on the cross-section ratio and flow division regime. It declares that counter-current flow arrangements with a cross-section ratio of  $K=0.7$  provides the highest heat transfer enhancement, especially with flow division regime 1.

It is worth comparing the heat transfer enhancements between the proposed counter-current channel and the double-pass channel proposed by Yeh et al. [27]. The comparison should be done for the geometrical case denoted by  $K=0.5$ . The ratio of the total heat transfer of the proposed counter-current channel to the total heat transfer of the double-pass channel [27] at three flow rates is listed in Table 2. Tabulated results show that the thermal performance of the proposed counter-current channel is less than that of the double-pass one at a low flow rate, but approaches to that at a high flow rate. The benefit of the proposed channel could be illustrated when comparing the power consumption increment and overall performance index.

**7-3- Power consumption**

Changing the flow passage within the two parallel plates may provide better thermal performance, but it may also

**Table 2. Thermal performance comparison between the proposed counter-current channel and double-pass channel [27]**

Gz	$(q_{cc}/q_{D.P})$
100	0.71
500	0.87
1000	1.0

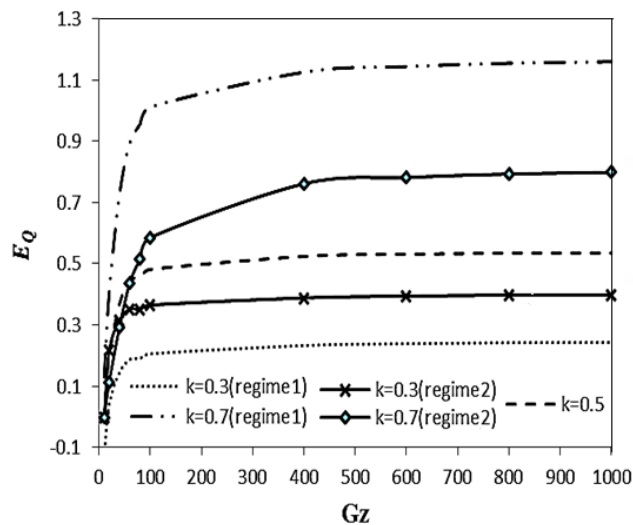


**Fig. 10. Heat transfer enhancement index of the counter-current channels at different flow rates**

increase the required power for supplying the same flow rate into the sub-channels. Therefore, another index should be introduced from the hydraulic viewpoint. The required power for pumping the prescribed volumetric flow rate within a typical channel is computed as

$$P = \sum \Delta p_i Q_i \tag{11}$$

where,  $\Delta p_i$  and  $Q_i$  are the pressure drop and the corresponding volumetric flow rate through each sub-channel. Then, the power consumption increment is defined as

$$E_p = \frac{P_{c.c} - P_s}{P_s} \tag{12}$$

The pressure drop through a typical parallel-plate channel with fully-developed laminar flow is simply computed [25]. Table 3 lists the power consumption increments of the proposed counter-current flow arrangement and also two already mentioned double-pass ones. The listed values declare an important performance of the proposed counter-current flow arrangement; the power consumption increment of the proposed flow arrangement is significantly less than those of the before investigated double-pass arrangements. It is favorable from the hydraulic viewpoint. Especially speaking,

the counter-current channel with cross-section ratio  $K=0.3$  and flow division regime 2 has the least power consumption increment among the other ones. But, as was mentioned in Fig. 10, it enhances the heat transfer less than those channels with greater cross-section ratios.

#### 7-4- Overall performance

It was illustrated that the proposed counter-current flow arrangement simultaneously increased the thermal performance and power consumption compared to the single-pass arrangement. Therefore, the overall performance of the new counter-current flow arrangement is introduced as

$$E_{overall} = \frac{w_Q E_Q}{w_P E_P} \tag{13}$$

where,  $w_Q$  and  $w_P$  are the suitable weighting factors, which should be identified by several considerations. In the absence of any consideration, they are selected as unity in the present study.

Fig.11 shows the overall performance index for all studied counter-current channels. Fig.11 shows that the overall performance of the counter-current channel increases rapidly at the low flow rates and then asymptotically approaches some invariant value depending on the cross-section ratio and

**Table 3. Comparison of the power consumption increment ( $E_p$ ) of the proposed counter-current channel with two different double-pass channels**

	$K=0.3$	$K=0.5$	$K=0.7$
Proposed counter-current channel, regime 1	11.175	9	36.766
Proposed counter-current channel, regime 2	8.048	9	13.762
Double-pass channel, Yeh et al. [27]	38.95	15	38.95
Double-pass channel, Goodarzi and Nouri [23]	47.7	39	150.06

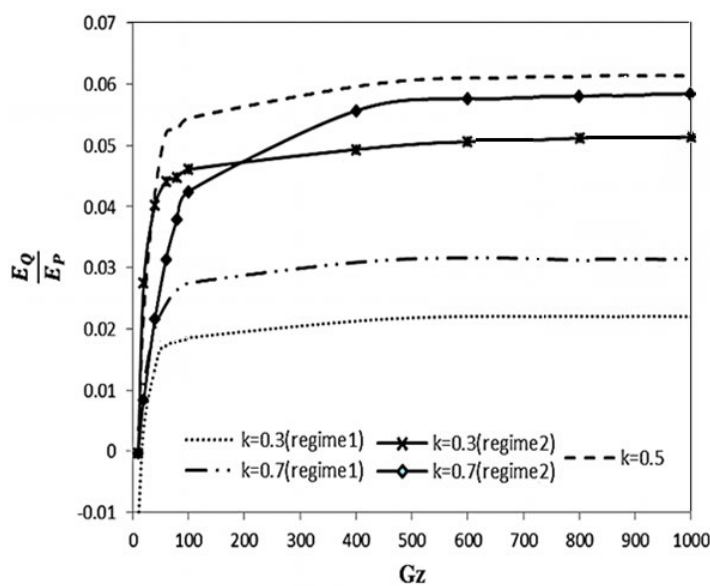


**Fig. 11. Overall performance index of the counter-current channels at different flow rates**

**Table 4. Percent of the overall performance improvement in the proposed counter-current channel relative to the double-pass channel [27]**

Gz	Percent of improvement
100	18%
500	45%
1000	67%

flow division regime. This Figure illustrates that the counter-current channel with cross-section ratio  $K=0.5$  has always the greatest overall performance index among the other ones. It is merely twice the overall performance of the counter-current channel with a crosssection ratio of  $K=0.7$  and flow division regime 1. Of course, the overall performance of the counter-current channel with a cross-section ratio  $K=0.7$  and flow division regime 2 is insignificantly less than that channel with  $K=0.5$  at high flow rate. Referring to Table 3, it is clear that the channel with  $K=0.7$  and flow division regime 2 has considerably low power consumption increment compared to the channel with  $K=0.5$ . Therefore, this flow arrangement may be more suitable than the channel with  $K=0.5$  at high flow rates.

Now the most important characteristic of the proposed counter-current channel could be presented. Comparing the overall performance between the proposed counter-current channel and double-pass one [27], illustrates that this index has been improved in the former. Table 4 lists the percentages of the overall performance improvement at the three mentioned flow rates. Tabulated results show greater improvement at a high flow rate.

**8- Conclusions**

A new counter-current flow arrangement has been proposed and investigated in the present study. Its thermal, hydraulic, and overall performances have been investigated compared to the benchmark single-pass arrangement and also double-pass arrangement. The obtained results illustrated that the proposed counter-current flow arrangement could improve thermal performance. Also, the power consumption for supplying the same flow rate into the counter-current flow arrangement increased, but the overall performance of the new counter-current flow arrangement was satisfactory for practical applications.

The most important characteristic of the proposed counter-current flow arrangement compared to the previously investigated double-pass arrangements is its less power consumption increment. Therefore, the proposed counter-current flow arrangement could be used as a good alternative for double-pass flow arrangements within the parallel-plate geometry with less power required to enhance the heat transfer.

**NOMENCLATURE**

$c_p$  heat capacity, J/kg.K

$E_p$  power consumption increment  
 $E_Q$  thermal improvement  
 $Gz$  Graetz number  
 $h$  convective heat transfer coefficient, W/m<sup>2</sup>.K  
 $k$  thermal conductivity, W/m.K  
 $K$  cross-section ratio  
 $L$  channel length, m  
 $Nu$  Nusselt number  
 $p$  pressure, Pa  
 $P$  power, W  
 $Pr$  Prandtl number  
 $q''$  heat flux, W/m<sup>2</sup>  
 $Q$  volumetric flow rate, m<sup>3</sup>/s  
 $Re$  Reynolds number  
 $T$  temperature, K  
 $U$  average velocity, m/s  
 $V$  velocity, m/s  
 $W$  channel width, m  
 $w_Q$  weight factor for percent of the thermal improvement  
 $w_p$  weight factor for power consumption increment  
 $x$  longitudinal coordinate, m  
 $y$  transverse coordinate, m

**Symbols**

$\theta$  dimensionless temperature  
 $\mu$  viscosity, kg/m.s  
 $\xi$  dimensionless longitudinal coordinate  
 $\rho$  density, kg/m<sup>3</sup>

**Subscriptions**

*c.c* counter-current channel  
*f.d* fullydeveloped condition  
*i* inlet  
*m* mean value  
*o* outlet  
*s* single-pass channel  
*total* total values  
*w* wall

**REFERENCES**

[1] R.K. Shah, A.L. London, Laminar Flow Convection in Ducts, Academic Press, New York, 1995.  
 [2] P.A. Ramachandran, Boundary integral solution method for the Graetz problem, Numerical Heat Transfer, Part B, 23 (1993) 257-268.  
 [3] A. Laouadi, N. Galanis, C.T. Nguyen, Laminar fully developed mixed convection in inclined tubes uniform heated on their outer surface, Numerical Heat Transfer, Part A, 26 (1994) 719-738.  
 [4] M.L. Michelsen, J. Villadsen, The Graetz problem with axial heat conduction, International Journal of Heat and Mass Transfer, 17 (1974) 1391-1402.  
 [5] E. Papoutsakis, D. Ramkrishna, H.C. Lim, The extended Graetz problem with prescribed wall flux, AIChE Journal, 26 (1980) 779-787.

- [6] S. Bilir, Numerical solution of Graetz problem with axial conduction, *Numerical Heat Transfer, Part A*, 21 (1992) 493-500.
- [7] B. Weigand, An exact analytical solution for the extended turbulent Graetz problem with Dirichlet wall boundary conditions for pipe and channel flows, *International Journal of Heat and Mass Transfer*, 39 (1996) 1625-1637.
- [8] C.H. Huang, M.N. Ozisik, Inverse problem of determining unknown wall heat flux in laminar flow through a parallel-plate duct, *Numerical Heat Transfer, Part A*, 21 (1992) 55-70.
- [9] A.V. Kuznetsov, L. Chang, M. Xiong, Effects of thermal dispersion and turbulence in forced convection in a composite parallel-plate channel: investigation of constant wall heat flux and constant wall temperature cases, *Numerical Heat Transfer, Part A*, 42 (2002) 365-383.
- [10] C.D. Ho, W.Z. Chen, J.W. Tu, Asymmetric wall heat fluxes boundary conditions in double-pass parallel-plate heat exchangers, *International Journal of Heat and Mass Transfer*, 52 (2009) 3555-3563.
- [11] L.D. Tijing, B.C. Pak, A study on heat transfer enhancement using straight and twisted internal fin inserts, *International Communications in Heat and Mass Transfer*, 33 (6) (2006) 719-726.
- [12] A. Sohankar, Heat transfer and fluid flow through a ribbed passage in staggered arrangement, *Iranian Journal of Science and Technology, Transaction B: Engineering*, 34 (B5) (2010) 471-485.
- [13] G. Wang, S.P. Vanka, Convective heat transfer in periodic wavy passages, *International Journal of Heat and Mass Transfer*, 38 (17) (1995) 3219-3230.
- [14] D.R. Sawyers, M. Sen, H.C. Chang, Heat transfer enhancement in three dimensional corrugated channel flow, *International Journal of Heat and Mass Transfer*, 41 (1998) 3559-3575.
- [15] J. Zhang, J. Kunda, R.M. Manglik, Effect of fin waviness and spacing on the lateral vortex structure and laminar heat transfer in wavy-plate-fin cores, *International Journal of Heat and Mass Transfer*, 47 (2004) 1719-1730.
- [16] H.M. Yeh, C.D. Ho, The improvement of performance in parallel-plate heat exchangers by inserting in parallel an impermeable sheet for double-pass operations, *Chemical Engineering Communications*, 83 (2000) 39-48.
- [17] C.D. Ho, W.S. Sheu, Double-pass heat or mass transfer through a parallel-plate channel with recycle, *International Journal of Heat and Mass Transfer*, 43 (2000) 487-491.
- [18] C.D. Ho, Y.J. Chuang, J.W. Tu, Double-pass flow heat transfer in a parallel-plate channel for improved device performance under uniform heat fluxes, *International Journal of Heat and Mass Transfer*, 50 (2007) 2208-2216.
- [19] C.D. Ho, J.W. Tu, C.M. Yang, Conjugated heat transfer in double-pass laminar counter flow concentric tube heat exchangers with sinusoidal wall fluxes, *International Journal of Heat and Mass Transfer*, 52 (2009) 45-55.
- [20] M. Goodarzi, S. Mazharmanesh, Heat transfer enhancement in parallel-plate double-pass heat exchanger using sinusoidal separating plate, *International Journal of Thermal Sciences*, 72 (2013) 115-124.
- [21] C.D. Ho, H.M. Yeh, Y.C. Tasi, Improvement in performance of multi-pass laminar counter flow heat exchangers with external refluxes, *International Journal of Heat and Mass Transfer*, 45 (2002) 3529-3547.
- [22] C.D. Ho, Y.C. Tasi, J.W. Tu, Heat transfer flow in a parallel-plate channel by inserting in parallel impermeable sheets for multi-pass coolers or heaters, *International Journal of Heat and Mass Transfer*, 47 (2004) 459-476.
- [23] M. Goodarzi, E. Nouri, A new double-pass parallel-plate heat exchanger with better wall temperature uniformity under uniform heat flux, *International Journal of Thermal Sciences*, 102 (2016) 137-144.
- [24] M. Goodarzi, S. Mazharmanesh, Analytical study on start-up process in parallel-plate channel under uniform heat flux, *International Journal of Thermal Sciences*, 94 (2015) 147-155.
- [25] S. Patankar, *Numerical Heat Transfer and Fluid Flow*, Hemisphere Publishing Corporation, McGraw-Hill, New York, 1980.
- [26] W.M. Kays, M.E. Crawford, *Convection heat and mass transfer*, 3<sup>rd</sup> ed., McGraw-Hill, New York, 1993.
- [27] H.M. Yeh, C.D. Ho, The Improvement of Performance in Parallel-plate Heat Exchangers by Inserting DM Parallel an Impermeable Sheet for Double-pass Operations, *Chemical Engineering Communications*, 183 (2000) 39-48.

#### HOW TO CITE THIS ARTICLE

M. Goodarzi, N. Eshghabadi, R. Sadeghi. *Improving Thermo-hydraulic Performance of Parallel-plate Flow with a Particular Counter-current Flow Division. AUT J. Mech Eng., 4(4) (2020) 481-492.*

DOI: [10.22060/ajme.2019.15507.5776](https://doi.org/10.22060/ajme.2019.15507.5776)



